Characteristics of sensitized emission in laser crystals

V. Lupei and A. Lupei
Institute of Atomic Physics, Institutul de Fizica şi Tehnologia Aparatelor cu Radiaţii, 76900 Bucharest, Romania

G. Boulon
Universite Claude Bernard, Lyon I, Laboratoire de Physico-Chimie des Matèriàux Luminescents, 69622 Villeurbanne, France
(Received 23 October 1995; revised manuscript received 1 February 1996)

The effects of sensitization on the static and dynamic behavior of the luminescence emission of donors (D) and acceptors (A) in codoped laser crystals are investigated. In many cases the sensitization with transition-metal ions of the weakly absorbing rare-earth laser emitters leads to the modification of the spectral properties of both D and A ions, due to the mutual crystal-field perturbations. The main modifications of the spectral properties due to the change of symmetry and/or strength of the crystal field acting on these ions are discussed. Due to the discrete nature of perturbations, the D and A systems become inhomogeneous and they could be separated in several homogeneous subsystems connected with specific D-A pairs along with the subsystem of ''isolated'' ions. The selective modifications of the energy-transfer processes due to the mutual static perturbations are the main subject of this paper. A theoretical modeling of the donor and acceptor emission kinetics in such complex systems is presented, assuming a discrete random uniform noncorrelated distribution. An essential point in the theoretical treatment is the fact that for nearest D-A pairs a mixed interaction picture, with strong influences of short-range ion-ion interactions must be considered. The codoping can lead to selective behavior of acceptor emission for various subsystems as concerns the wavelength, the moment and peak instantaneous emission, and the character of the subsequent decay. The model is illustrated with data on the $^3H_4$ Tm^{3+} emission in YAG sensitized with Cr^{3+} or Fe^{3+}. [S0163-1829(96)04922-3]

I. INTRODUCTION

An important way to improve the efficiency of the solid-state lasers is the sensitization of emission of weakly absorbing active ions with other ions whose absorption better matches the pump emission spectrum and which are able to transfer the excitation to the activator. A fast energy transfer from sensitizer (donor, D) to the activator (acceptor, A) is claimed in order to avoid the loss of excitation by intrinsic donor processes (emission or multiphonon relaxation). Accordingly, the efficiency of the energy transfer to the acceptor is determined by the balance between the deexcitation of the donor in the presence of transfer as compared with these intrinsic processes.

The energy-transfer characteristics could be determined from the temporal behavior of the emission intensity of the sensitizer and activator ions after a short laser-pulse excitation of the donor levels. Traditionally, the systems of sensitizer and activator ions are considered as homogeneous, all the members of each system having identical spectral and temporal (radiative) properties. In presence of direct D-A energy transfer, the donor emission decay is affected by a multiplicative factor $\exp[-P(t,C_A)]$, which expresses the probability, averaged over the entire ensemble of acceptor ions, that the donor is not deexcited at the moment of time t by transfer to any of the acceptor ions from the system. $P(t,C_A)$ is a transfer function which depends on time and on the relative acceptor concentration C_A; this dependence can be determined for given models of acceptor ions distribution in the host lattice if the transfer rate $W(r_i)$ to any acceptor i placed at a distance r_i from a donor is known. The individual rates $W(r_i)$ depend on the nature of the interaction between the donor and the acceptor i and can be expressed[1] as a product between a microparameter of interaction C_{DA} and a function on distance r_i. The microparameter C_{DA} depends on the spectroscopic properties of the D and A ions, such as the superposition integral of donor emission and acceptor absorption, the acceptor integral absorption cross section and the lifetime of donor intrinsic emission; in case of the homogeneous D and A systems the microparameter C_{DA} for a given interaction is considered as a constant. The various D-A interactions impose specific dependences of $W(r_i)$: in the case of the multipolar interactions this is given by r_i^{-s}, with $s=6$, 8 or 10 for dipole-dipole, dipole-quadrupole, and quadrupole-quadrupole interactions, respectively, while the superexchange interactions lead to a very strong dependence on distance but also on the nature, number, and geometrical configuration of the ligands intervening between the D and A ions. The most popular distribution models used for calculation of the functional form of $P(t,C_A)$ are based either on a continuous uniform[1–3] or a discrete random and equiprobable[4] occupancy of sites. The temporal evolution of acceptor emission after a short pulse excitation of the donor is a curve with rise and fall, the first part being determined by the fastest and the second by the slowest of the two processes: the feeding with excitation from donor (which is determined both by the donor intrinsic deexcitation and by the rate of energy transfer) and the acceptor deexcitation.

The need for a high transfer efficiency implies large transfer rates $W(r_i)$ and thus favors the systems with short D-A distances and with a good packing of the acceptor sites around the donors. Recent spectroscopic investigations[5–11] show that, due to their dimensional mismatch with the host cations, the D and A ions could produce strong mutual asymmetric crystal-field perturbations at each other's site, func-

tion on distance r_i, and on the relative direction of perturbation with respect to the local symmetry axes of the D and A centers. These static perturbations could modify the symmetry and/or the strength of the crystal field acting on these ions, leading to an additional rise of the energy levels degeneracy, the shift of the energy levels and modification of their relative positions, the alteration of the selection rules, and of the radiative transition probabilities. The most intense perturbations take place for the near D-A pairs; due to the strong distance and orientation dependence of the perturbation and to the discreteness of the crystalline lattice, the perturbations corresponding to several types of such near D-A pairs form a discrete chain and could produce resolvable spectroscopic effects, while the perturbing effect of the most distant ions reduces to an inhomogeneous broadening of the spectral lines. The presence of the strongly perturbed centers is made evident by the apparition of spectral satellites; thus the homogeneous D and A systems are transformed into inhomogeneous systems, composed of homogeneous subsystems corresponding to the spectrally resolved D-A pairs, an additional subsystem being composed by the D or A ions for which the effect of perturbations is not resolved (the subsystem of ''isolated'' ions).

The specific modifications of the spectral properties of the perturbed D and A subsystems lead[12] to selective changes of their energy-transfer properties: the microparameters C_{DA} for the various interactions may cease to be a constant for the whole D and A systems but they will take individual values for each subsystem. This individualization is enhanced by the possibility of having specific multiple interacting situations as well as by the fact that distribution of acceptors around the donor and the averaging of the transfer rates over the ensembles of acceptors are specific for each of the D-A subsystems.

The present paper investigates the effect of these static perturbations on the energy transfer and on activator emission properties for subsystems with direct D-A energy transfer without preliminary migration on donors and without back transfer from A to D ions. We also disregard the intrasystem (D or A) perturbing effects due to statistical ensembles (pairs, triads and so on) of dopant ions of a given sort in near-neighbor lattice sites. The rate equation modeling of the sensitized emission of the activators, coupled with the statistical probability of occurrence for the various subsystems shows that it is complex and heterogeneous. The model is illustrated for the $^3H_4$ Tm^{3+} emission in YAG crystals sensitized by Cr^{3+} and Fe^{3+}.

II. THEORY

Assuming that the largest number of resolved independent satellites in the optical spectra of D or A ions is k, the inhomogeneous systems of D and A ions could be divided into $l=k+1$ homogeneous subsystems. The relative concentrations of these subsystems could be calculated for given models of distribution of D and A ions in the available lattice sites. When the D and A ions have identical electric charge with the substituted host cations and in absence of dimensional correlation, this distribution could be considered as discrete, random, and equiprobable. If the perturbation depends only on the D-A distance, the nearest perturbing ion could be considered as placed on a coordination sphere of radius r_i around the perturbed ion; for radii larger than r_k the perturbing effect is no longer resolved. If a coordination sphere of acceptor ions around a donor ion contains m_{Aj} available sites, the probability of having n_{Aj} of these occupied by A ions depends on their relative concentration in crystal, C_A:

$$N_{DAj}(m_{Aj},n_{Aj})=\frac{m_{Aj}!}{n_{Aj}!(m_{Aj}-n_{Aj})!}C_A^{n_{Aj}}(1-C_A)^{m_{Aj}-n_{Aj}}. \tag{1}$$

A similar relation holds for the probability of having D ions near a given A ion. In the case of the D-A pairs, $n_{Aj}=1$ and Eq. (1) can be used to calculate the absolute concentration of a given D-A pair subsystem, $n_D N_{DAj}(m_{Aj},l)$. Equation (1) shows that even for very low C_A (or C_D) concentrations there is a finite probability of having near D-A pairs. In what follows, for the sake of simplicity, we assume that C_A and C_D are low enough so we can neglect the probabilities of occurrence for ensembles larger than pairs, and inside the perturbation sphere of radius r_k there is only one perturbing ion j; we also neglect the intrasystem perturbative effects.

A. The donor emission

In the presence of energy transfer, the emission of the donor subsystems D_l, $l=1,\ldots,k+1$ is given by

$$I_{Dl}(t)=n_{Dl}(0)A_{Dl}^{(e)}\exp\left(-\frac{t}{\tau_{Dl}}\right)\exp[-P_{DlA}(t)] \tag{2}$$

where $n_{Dl}(0)$ is the number of donors from the system D_l excited at $t=0$, $A_{Dl}^{(e)}$ is their spontaneous emission coefficient, τ_{Dl} is the lifetime of donors D_l at very low acceptor concentrations, and $P_{DlA}(t)$ is the energy-transfer function. As discussed above this function can be determined for a given model of distribution of the acceptor ions over the lattice sites available to them. Due to the discrete character of the perturbations and to the importance of near D-A pairs, the most suitable distribution model of donor and acceptor ions in our case is that based on a discrete occupancy of the specific crystallographic sites; we also assume that the D and A substitution is random and equiprobable, with probabilities equal to the relative concentrations of donors or acceptors, C_D and respectively C_A. In this case the energy-transfer function can be generally written as[4]

$$P_{DlA}(t)=\sum_i \ln\{1-C_A+C_A\exp[-W_{DlA}(\mathbf{r}_i)t]\} \tag{3}$$

with the sum extended on all the sites available to acceptors. This function can be also written as

$$P_{DlA}(t)=\sum_h m_h\ln\{1-C_A+C_A\exp[-W_{DlA}(\mathbf{r}_h)t]\}, \tag{4}$$

where the sum is now performed on the coordination spheres containing each m_h equivalent sites.

The decay equation (2) could be particularized for each D subsystem. Thus, for the perturbed donor subsystems D_j the probability of having an acceptor ion on sphere r_j and inside the perturbation sphere is equal to one; by denoting

the transfer rate to the particular perturbing acceptor by $W_{DjAj}(\mathbf{r}_j)$, the global energy-transfer function for these perturbed donor subsystems can be written

$$P_{DjA}(t)=W_{DjAj}(\mathbf{r}_j)t+P_{DjA}^{(d)}(t), \tag{5}$$

where $P_{DjA}^{(d)}(t)$ describes the transfer to distant acceptors, outside of the perturbing sphere,

$$P_{DlA}^{(d)}(t)=\sum_{i>N_{Ak}} \ln\{1-C_A+C_A\exp[-W_{DlA}(r_i)t]\}$$
$$=\sum_{h>k} m_{Ah}\ln\{1-C_A+C_A\exp[-W_{DjA}(r_h)t]\} \tag{6}$$

and $N_{Ak}=\Sigma_j m_{Aj}$. The emission decay of donors from the unperturbed subsystem D_n is affected only by the transfer to distant acceptors and the transfer function is similar to (6). The sum in (6) spans the acceptor sites from all subsystems, including the perturbed acceptor centers which are farther than r_k from the excited donor. For the range of dopant concentrations usual in laser techniques, the global energy-transfer functions $P_{DlA}(t)$ could be approximated by a sum of transfer functions to the individual acceptor subsystems

$$P_{DlA}(t)=\sum_f P_{DlAf}(t) \quad \text{with} \quad f=1,\ldots,k+1 \tag{7}$$

with

$$P_{DjAj}(t)=W_{DjAj}(\mathbf{r}_j)t+\sum_{i>N_{Ak}} \ln\{1-C_{Aj}$$
$$+C_{Aj}\exp[-W_{DjAj}(\mathbf{r}_i)t]\}$$
$$=W_{DjAj}(\mathbf{r}_j)t+P_{DjAj}^{(d)}(t), \tag{8}$$

while

$$P_{DjAn}(t)=P_{DjAn}^{(d)}$$
$$=\sum_{i>N_{Ak}} \ln\{1-C_{An}+C_{An}\exp[-W_{DjAn}(\mathbf{r}_i)t]\}. \tag{9}$$

C_{Aj} and C_{An} are the relative concentrations of the perturbed and unperturbed acceptor subsystems.

According to Eq. (5) in the case of the perturbed donor subsystems the transfer function contains two terms, the first describing the transfer to the perturbing acceptor companion of the excited donor and the second accounting for the transfer to distant acceptors. Since the perturbation is produced by near ions, the first of these transfers is very fast and it could be governed by a multiple interaction including superexchange and various multipolar interactions. As discussed in the Introduction, the microparameters of the multipole interactions for these centers could be modified from those corresponding to distant *D*-*A* pairs due to the change of the spectroscopic properties of the *D* and *A* ions and the transfer rates may not show clear distance dependences for the different perturbed subsystems. In many cases, the rates corresponding to the nearest-neighbor *D*-*A* pairs are dominated by superexchange and their value is so high that the emission of the corresponding perturbed donor ions is almost completely quenched. The second term of (5) which describes the transfer to distant acceptors, contains a truncated sum, which excludes all the sites inside the perturbation sphere; thus, due to the strong dependence on distance, the individual transfer rates inside this sum are small and the transfer is much slower. However, the presence of this second term shows that, contrary to common belief, the emission decay of donors in the near *D*-*A* pairs is not exponential and it depends on the acceptor concentration; this dependence is more evident when the rate $W_{DjAj}(r_j)$ is not very large. The emission of the unperturbed donor subsystem contains only the slow transfer described by the truncated sum.

The number of emitting donor centers at $t=0$ in each of the subsystems D_l is

$$n_{Dj}(0)=n_{Dj0}A_{Dj}^{(a)}=n_{D0}m_{Aj}C_A(1-C_A)^{m_{Aj}-1}A_{Dj}^{(a)}, \tag{10}$$

$$n_{Dn}(0)=n_{Dn0}A_{Dn}^{(a)}=n_{D0}[1-(1-C_A)^{N_k}]A_{Dn}^{(a)}, \tag{11}$$

where n_{Dj0} is the total number of donors from the subsystem j, $A_{Dj}^{(a)}$ is the pump absorption coefficient for donors D_j, and n_{D0} is the total number of donor ions.

If the excitation of the donor system is nonselective and the emission from the whole donor system is monitored, it contains contributions from all the subsystems discussed above:

$$I_D(t)=\sum_l I_{Dl}(t)$$
$$=\sum_l n_{Dl0}A_{Dl}^{(e)}\exp\left(-\frac{t}{\tau_{Dl}}\right)\exp[-P_{DlA}(t)]. \tag{12}$$

By taking into account the possible differences between the values of $A_{Dl}^{(a)}$,$A_{Dl}^{(e)}$, and τ_{Dl} and the peculiarities of the transfer functions for the various subsystems it is now apparent that the temporal evolution of the global emission of inhomogeneous donor systems is very complex and it could show large differences from the case of homogeneous systems.

B. Acceptor emission

The acceptor ions from the perturbed A_g (with $g=1,\ldots,k$) subsystems could be excited by a fast transfer from the perturbing excited donor companion as well as by slow transfer from the other donors, regardless to which subsystem D_l they belong; at the same time the acceptors of the unperturbed subsystem A_n can be excited only by distant donors. The temporal evolution for the populations of acceptor subsystems are then obtained by solving the rate equations

$$\frac{dn_{Ag}}{dt}=-\frac{n_{Ag}}{\tau_{Ag}}-n_{Ag}\frac{dP_{AgA}}{dt}+n_{Dg}W_{gg}+\sum_j n_{Dj}\frac{dP_{DjAg}^{d}}{dt}$$
$$+n_{Dn}\frac{dP_{DnAg}(t)}{dt}, \tag{13}$$

$$\frac{dn_{An}}{dt}=-\frac{n_{An}}{\tau_{An}}-n_{An}\frac{dP_{AnA}}{dt}+\sum_j n_{Dj}\frac{dP^d_{DjAn}}{dt}+n_{Dn}\frac{dP_{DnAn}}{dt},\tag{14}$$

where P_{AgA} and P_{AnA} describe the possible processes of deexcitation of acceptor subsystems by cross relaxation with ions from any acceptor subsystem. The solutions of (13) and (14) are

$$\begin{aligned}n_{Ag}(t)=&\exp\left[-\left(\frac{t}{\tau_{Ag}}+P_{AgA}(t)\right)\right]\\&\times\left\{n_{Dg}(0)W_{DgAg}\int_0^t\exp\left[\frac{s}{\tau_{Ag}}-\left(\frac{1}{\tau_{Dg}}+W_{DgAg}\right)s\right]\right.\\&\times\exp[P_{AgA}(s)-P^{(d)}_{DgA}(s)]ds\\&+\sum_j n_{Dj}(0)\int_0^t\exp\left[\frac{s}{\tau_{Ag}}-\left(\frac{1}{\tau_{Dj}}+W_{DjAj}\right)s\right]\\&\times\exp[P_{AgA}(s)-P^{(d)}_{DjA}(s)]\frac{dP^{(d)}_{DjAg}(s)}{ds}ds\\&+n_{Dn}(0)\int_0^t\exp\left[\frac{s}{\tau_{Ag}}-\frac{s}{\tau_{Dn}}\right]\exp[P_{AgA}(s)\\&\left.-P_{DnA}(s)]\frac{dP_{DnAg}(s)}{ds}ds\right\}\end{aligned}\tag{15}$$

and

$$\begin{aligned}n_{An}(t)=&\exp\left[-\left(\frac{t}{\tau_{An}}+P_{AnA}(t)\right)\right]\\&\times\left\{\sum_j n_{Dj}(0)\int_0^t\exp\left[\frac{s}{\tau_{An}}-\left(\frac{1}{\tau_{Dj}}+W_{DjAj}\right)s\right]\right.\\&\times\exp[P_{AnA}(s)-P^{(d)}_{DjA}(s)]\frac{dP^{(d)}_{DjAn}(s)}{ds}ds\\&+n_{Dn}(0)\int_0^t\exp\left[\frac{s}{\tau_{An}}-\frac{s}{\tau_{Dn}}\right]\\&\left.\times\exp[P_{AnA}(s)-P_{DnA}(s)]\frac{dP_{DnAn}}{ds}ds\right\}.\end{aligned}\tag{16}$$

Equations (15) and (16) describe the evolution of the populations of the acceptor subsystems under nonselective pumping in the donor system and they reflect the contribution of the energy transfer from the various donor subsystems. The first term on the right side of Eq. (15) describes the excitation of the acceptors A_g by transfer from the adjacent excited donors D_g, the second term describes the effect of distant transfer from any perturbed donor subsystem (the sum over j includes g), while the third term describes the distant transfer from the unperturbed donors D_n. Equations (15) and (16) could be used to describe the emission under selective pump in any of the donor subsystems by a proper choice of the excited donor concentrations $n_{Dl}(0)$. At the same time, the total acceptor emission under nonselective excitation in the donor system is given by $\Sigma_g n_{Ag}(t)A^{(e)}_{Ag}+n_{An}(t)A^{(e)}_{An}$, where $A^{(e)}_{Ag}$ and $A^{(e)}_{An}$ are the spontaneous emission coefficients for the various acceptor subsystems.

Generally, due to the complex form of the transfer functions, the integrals in Eqs. (15) and (16) cannot be expressed analytically; this makes the analysis of these equations very difficult. However, if the transfer functions are approximated by linear functions of time, $P_{DmAn}(t)=C_{An}W_{DmAn}t$, one has

$$\begin{aligned}n_{Ag}(t)=&\frac{n_{Dg}(0)W_{DgAg}}{W^{(t)}_{AgA}-W^{(t)}_{DgA}}[\exp(-W^{(t)}_{DgA}t)\\&-\exp(-W^{(t)}_{AgA}t)]\\&+\sum_j\frac{C_{Ag}n_{Dj}(0)W^{(d)}_{DjAg}}{W^{(t)}_{AgA}-W^{(t)}_{DjA}}[\exp(-W^{(t)}_{DjA}t)\\&-\exp(-W^{(t)}_{AgA}t)]\\&+\frac{C_{Ag}n_{Dn}(0)W^{(d)}_{DnAg}}{W^{(t)}_{AgA}-W^{(t)}_{DnA}}[\exp(-W^{(t)}_{DnA}t)\\&-\exp(-W^{(t)}_{AgA}t)]\end{aligned}\tag{17}$$

and

$$\begin{aligned}n_{An}(t)=&\sum_j\frac{C_{An}n_{Dj}(0)W^{(d)}_{DjAn}}{W^{(t)}_{AnA}-W^{(t)}_{DjA}}[\exp(-W^{(t)}_{DjA}t)\\&-\exp(-W^{(t)}_{AnA}t)]\\&+\frac{C_{An}n_{Dn}(0)W^{(d)}_{DnAn}}{W^{(t)}_{AnA}-W^{(t)}_{DnA}}[\exp(-W^{(t)}_{DnA}t)\\&-\exp(-W^{(t)}_{AnA}t)],\end{aligned}\tag{18}$$

where

$$W^{(t)}_{AlA}=\frac{1}{\tau_{Al}}+C_AW_{AlA},$$

$$W^{(t)}_{DjA}=\frac{1}{\tau_{Dj}}+W_{DjAj}+\sum_l C_{Al}W^{(d)}_{DjAl},$$

$$W^{(t)}_{DnA}=\frac{1}{\tau_{Dn}}+\sum_l C_{Al}W^{(d)}_{DnAl}.$$

The contributions of the energy transfers from the various donor subsystems to the emission of acceptors is described in Eqs. (17) and (18) by functions of type

$$n(t)=\frac{n_D(0)W_{DA}}{W_A-W_D}[\exp(-W_Dt)-\exp(-W_At)],\tag{19}$$

where W_D and W_A describe the global decay of donor and of acceptor systems, respectively, and W_{DA} describes the energy transfer between these systems. The function $n(t)$ given by Eq. (19) is a curve with rise and fall: it starts from zero at $t=0$, reaches a maximal value

$$n_{A\,\max}=\frac{n_D(0)W_{DA}}{W_D}\left(\frac{W_A}{W_D}\right)^{W_A/(W_D-W_A)} \tag{20}$$

at the moment

$$t_{A\,\max}=\frac{\ln(W_A/W_D)}{W_A-W_D}, \tag{21}$$

then decays in time. The decay part is mainly determined by the smallest of the rates (W_A, W_D). The integral number of acceptor ions excited by transfer is

$$n_{A\,\mathrm{tot}}=\frac{n_D(0)W_{DA}}{W_D W_A}. \tag{22}$$

With these relations we can estimate the effect of transfer on the evolution of acceptor emission. Thus, if we take as model data $\tau_D^{-1}\approx 10^3\ \mathrm{s}^{-1}$ and $W_A\approx 10^4\ \mathrm{s}^{-1}$, if the energy transfer is very fast, $(W_{DA}\approx 10^7\ \mathrm{s}^{-1})$, $n_{A\,\max}$ equals $0.993n_D(0)$ and occurs at 0.69 μs after excitation; the rise is determined by the fast decay of the donor due to the energy transfer, while the decay portion is determined by the intrinsic decay of the acceptor system. If the roles of deexcitation mechanisms of the donor systems are interchanged, i.e., if $\tau_D^{-1}\approx 10^7\ \mathrm{s}^{-1}$ and $W_{DA}\approx 10^3\ \mathrm{s}^{-1}$ the evolution of $n_A(t)$ will be similar to the previous case, but $n_{A\,\max}$ and $n_{A\mathrm{tot}}$ will be much smaller, by about four orders of magnitude; this shows that the energy-transfer rate W_{DA} determines the amplitude of $n_A(t)$, while its shape and $t_{A\,\max}$ are determined by the whole process of deexcitation W_D of the donor system and by its relation to W_A. For a moderate transfer rate, for instance $W_{DA}\approx 2\times 10^4\ \mathrm{s}^{-1}$, $n_{A\,\max}$ will be only $0.4852n_D(0)$, but $t_{A\,\max}=67.5$ μs and the decay portion is still determined by the acceptor intrinsic deexcitation. If the transfer is very slow, $W_{DA}\approx 10^3\ \mathrm{s}^{-1}$, the peak instantaneous acceptor excitation is low, $n_{A\,\max}=0.067n_D(0)$, $t_{A\ \max}=201$ μs and the decay portion of $n_A(t)$ is determined by the deexcitation of the donor system (intrinsic and by energy transfer).

When using these conclusions, the relative concentrations of the various donor subsystems must be taken into account. The first term of Eq. (17) describes the excitation of the perturbed acceptor A_g by fast energy transfer from its companion D_g; due to the very high transfer rates in the perturbed D-A pairs the peak instantaneous excitation of A_g is high despite the usually low concentration of the perturbed donor subsystem D_g; at large D and A concentrations it could overpass that of the unperturbed acceptor subsystem A_n. The second term of (17) describes the excitation due to the slow transfer from distant perturbed centers; although the transfer is slow and thus determines a very low amplitude of excitation, due to fast deexcitation of these perturbed donor centers by transfer to their near companions, the time $t_{A\,\max}$ for this term is short, similar to that of the first term. The third term, which describes the transfer from the unperturbed donor subsystem, leads to a slow excitation of low amplitude which is, in a given degree, compensated by the high concentration of this donor subsystem. The global emission of each perturbed acceptor subsystem under nonselective pump in the donor system consists of a sharp increase to a high instantaneous value, followed by a decay described by the acceptor deexcitation; a late shoulder on this decay could occur due to the slow excitation described by the third term in (17). In case of the nonperturbed acceptor subsystem A_n, Eq. (18) predicts a fast but very weak excitation due to the distant transfer from the perturbed donor subsystems, followed by a slow but much stronger excitation from the unperturbed donor subsystem.

This complex behavior of excitation of the acceptors by energy transfer makes possible higher peak instantaneous excitation of the perturbed acceptors as compared to the unperturbed ones although the concentration of the latter is much larger. Also, since the energy transfer and intrinsic deexcitation processes of the various D and A subsystems could have different temperature or concentration dependences, the acceptor excitation picture could change in various conditions of experiment. Numerical calculations with the exact Eqs. (15) and (16) show that the general features of excitation, described in the approximation of linear temporal dependence of the transfer functions are preserved.

While the peak instantaneous emission values for identical $n_D(0)$ values in the case of rapid, moderate, and slow energy transfer show very large differences, the total number of acceptors excited by energy transfer $n_{A\,\mathrm{tot}}$, Eq. (22), by using the model rate values as above amounts to $0.999\times 10^{-5}n_D(0)$, $0.952\times 10^{-5}n_D(0)$, and $0.5\times 10^{-5}n_D(0)$, respectively, for the three cases of transfer. Thus as concerns the absolute value of the total sensitized emission for the various acceptor subsystems considered here, their relative concentrations play a more important role than for the peak instantaneous values: usually this emission is larger for the unperturbed acceptor subsystem than for the perturbed ones, although at high D and A concentrations the situation might be reversed.

III. EMISSION OF $^3H_4$ Tm^{3+} IN Cr^{3+} OR Fe^{3+}-SENSITIZED GARNETS

The considerations of the previous sections can be illustrated for Cr^{3+} or Fe^{3+}-sensitized $^3H_4$ emission of Tm^{3+} in garnets. Tm^{3+} is an important 2 μm laser emitter from the $^3F_4$ level which is populated from $^3H_4$ by a cross relaxation $(^3H_4, {}^3H_6)\rightarrow(^3F_4, {}^3F_4)$; this imposes high concentrations up to about 5–6 at. %. The low Tm^{3+} absorption in the spectral ranges of the existing strong pumping sources precludes a high laser efficiency for the systems doped only with Tm^{3+}. However, an efficient sensitization of these systems was obtained by codoping the garnet crystals with Cr^{3+} (which transfers the energy to the $^3F_2$ and $^3F_3$ Tm^{3+} levels)[6–8,13–15] or with Fe^{3+} in tetrahedral sites, which transfer the energy to $^3H_4$ directly.[9,10] The high Tm^{3+} content determines large concentrations for the perturbed donor subsystems.

For this investigation we used Czochralski grown crystals of yttrium aluminum garnet (YAG) or gadolinium gallium garnet (GGG) activated with Tm^{3+} (up to 5 at. %) and sensitized with Cr^{3+} (up to 1 at. %) or Fe^{3+} (up to 5 at. %). The donor (Cr^{3+} or Fe^{3+}) and acceptor ($^3H_4$ Tm^{3+}) emission was measured from 4.2 to 300 K under excitation with the second harmonic of YAG:Nd (532 nm) or with excimer—or YAG:Nd—pumped dye lasers and the emission was analyzed by using high-resolution monochromators and

processed either by using boxcar or photon counting techniques. Since for YAG the spectral resolution is better, the main discussion of the results will be concentrated on this crystal.

A. Spectroscopic properties of single-doped Tm^{3+} garnets

The spectroscopic properties of Tm^{3+} ions in garnets have been investigated in the last few years to obtain correct energy-level diagram for prevailing centers N, Tm^{3+} in nonperturbed dodecahedral c sites of D_2 point symmetry.[16–18] For Tm^{3+} in D_2 symmetry the dipole transitions between crystal-field components labeled by identical representations are forbidden and the corresponding lines are missing from the optical spectra. In all symmetries lower than D_2 the forbiddeness of the $\Gamma_i(J') \rightarrow \Gamma_i(J'')$ transitions is raised. Besides N centers, the Tm^{3+} spectra contain a rich structure of satellites. Up to six satellites, whose intensity with respect to that of the main center N does not change with Tm^{3+} concentration, have been observed in YAG,[19] but only three in GGG. These satellites could be connected with the presence of lattice defects in the vicinity of the Tm^{3+} ion, most probably the nonstoichiometric excess of Y^{3+} ions in YAG (about 1.7–2 %) or Gd^{3+} in GGG (about 7%) which substitute the much smaller Al^{3+} ions, respectively, Ga^{3+} in octahedral a sites.[20] From symmetry considerations, up to three different such perturbations could be produced by $Y^{3+}(a)$ or $Gd^{3+}(a)$ defect centers from the first coordination sphere and another three from the second sphere[20] at the Tm^{3+} c site. Such satellites, traditionally labeled by P, have been observed in many rare-earth optical spectra as, for instance Er^{3+} (Refs. 20 and 21) or Nd^{3+} (Refs. 20, 22, and 23) in YAG, Er^{3+} (Ref. 20) or Pr^{3+} (Ref. 24) in GGG. The three possible perturbations due to a $Y^{3+}(a)$ defect center in the first coordination sphere are not equal in strength and sign. For the most perturbed center P of Tm^{3+} in YAG, the optical spectra are richer than for the nonperturbed N center, showing that a sizable lowering of the crystal-field symmetry takes place. No satellites could be unambiguously assigned to Tm^{3+} pairs in YAG or GGG, although the optical spectra of large rare-earth ions such as Nd^{3+} (Refs. 20, 22, and 23) in YAG or Pr^{3+} (Ref. 24) in GGG show the presence of satellites due to ion pairs; this can be explained by the weak lattice distortion introduced by doping with Tm^{3+}.

The emission decay of the $^3H_4$ Tm^{3+} level after short pulse pumping in $^3F_3$ is complex and depends on Tm^{3+} concentration and on temperature. At very low Tm^{3+} concentrations this decay is exponential with a lifetime of 560 μs, over the entire range of temperatures from 4.2 to 300 K. With increasing Tm^{3+} concentration, the decay becomes nonexponential. The processes of concentration quenching of this level emission, important in feeding $^3F_4$ 2 μm metastable laser level are not completely understood. Besides the direct energy transfer by cross relaxation the migration might contribute to emission decay. The ion-ion interaction responsible for transfer at low activator concentrations (up to 2–3 at. %) is dipolar for the distant Tm-Tm pairs, as suggested by the $t^{1/2}$ dependence of decay at long times, but the faster drop at early times indicates a short-range interaction (probably quadrupole-quadrupole as suggested in Ref. 25) for the near Tm-Tm pairs; at high concentrations, this interaction could dominate the entire decay.

B. Tm^{3+} emission in Cr^{3+} sensitized garnets

Cr^{3+} occupy only the octahedral a sites of garnets. Codoping of the garnet crystals with Tm^{3+} and Cr^{3+} determines the apparition of new satellites in the Tm^{3+} optical spectra.[6,8] In YAG:Tm^{3+},Cr^{3+} three such new satellites are observed in the $^3H_4$ Tm^{3+} level: C_1 at 793.42 nm, C_2 at 793.24 nm and C_3 at 793.06 nm, while the nonperturbed center N is at 793.35 nm.[8] By similarity with P centers, these new satellites have been assigned to three different perturbations produced by $Cr^{3+}(a)$ ions from the first coordination sphere at the c site occupied by Tm^{3+}. However, the possibility of connecting these satellites with the perturbing effect of Cr^{3+} ions in the first, second, and third coordination spheres around Tm^{3+} might be also taken into account. The spectra of centers C_1 and C_2 are similar to that of center N, excepting the shifts of the lines, while the satellite C_3 corresponds to a stronger perturbation, manifested by a larger energy shift and the apparition of additional lines corresponding to transitions forbidden in the D_2 symmetry, such as the $^3H_4(1) \rightarrow {}^3H_6(2)$ emission line between two Γ_1 states. The transition probabilities for all other lines of this center could be also modified, with a possible change of the radiative lifetime for Cr^{3+} and Tm^{3+}. The satellites C_i are well resolved in the Tm^{3+} emission at low temperatures, but with increasing temperature the lines broaden and the resolution is gradually lost: at 77 K the satellite C_3 could be still resolved, but C_1 and C_2 lines overlap with N. We note also that the Tm^{3+} lines in YAG:Cr,Tm are broader than in single-doped crystals, due probably to an inhomogeneous broadening produced by perturbations of distant Cr^{3+} ions. No satellites due to Tm^{3+} codoping were observed in the Cr^{3+} spectra, even in the narrow R lines.

The Tm^{3+} emission in the codoped YAG:Cr,Tm crystals can be excited by energy transfer from Cr^{3+} by pump in the broad $^4T_1$ or $^4T_2$ bands or in the narrow R_1 and R_2 lines. Depending on Cr^{3+} and Tm^{3+} concentration, pump wavelength, and moment of registration after the exciting pulse, the Cr^{3+} sensitized Tm^{3+} emission could be dominated, at low temperatures, by these three new satellites.[8] Figure 1 shows part of the $^3H_4$ Tm^{3+} emission of a YAG:Cr (0.2 at. %) Tm (3.1 at. %) sample under pumping in the Cr^{3+} R_2 line at 4.2 K with a wavelength which, for a registration delay of 2 μs, leads to a similar intensity emission for the three C_1 Tm^{3+} satellites; the transition $^3H_4(1) \rightarrow {}^3H_6(2)$ for C_3 is also shown. The 532 nm nonselective pumping at 4.2 K in the $^4T_2$ band leads to the emission of the three centers: the emission of center N is weak at early times but it gains importance at long times after excitation. The excitation spectra of the C_i Tm^{3+} centers in the region of Cr^{3+} R lines show clearly that the peaks of excitation for these satellites are different and they do not coincide with the nonperturbed R lines. By tuning finely the wavelength of excitation inside the R lines, the ratios of emission intensities of the C_i Tm^{3+} centers could be drastically changed. The presence of these three new C_i satellites in Tm^{3+} spectra gives

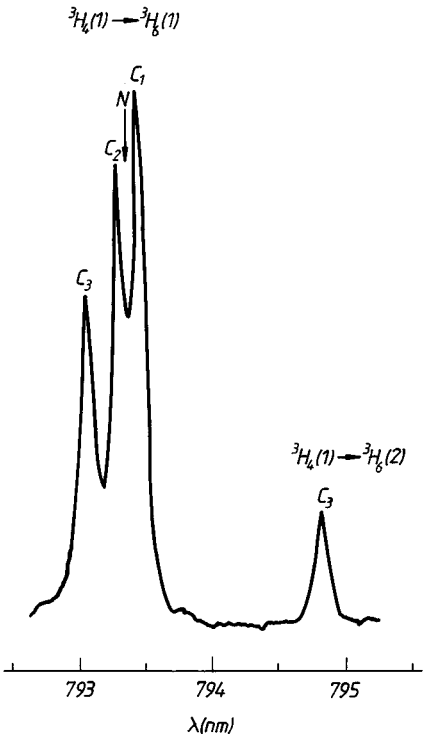

FIG. 1. Part of the $^3H_4 \rightarrow {}^3H_6$ Tm^{3+} emission of a YAG: Cr(0.2 at. %), Tm(3.1 at. %) under quasiselective pumping in the R_2 Cr^{3+} line.

grounds to divide the systems of activators (Tm^{3+}) and sensitizer (Cr^{3+}) into four subsystems (C_1, C_2, C_3, N).

Under selective excitation in the $^3F_2$ or $^3F_3$ Tm^{3+} levels, the $^3H_4$ emission decay in YAG: Cr, Tm is similar for all these centers (C_i and N), however, under quasiselective dye pump in the Cr^{3+} R lines or under nonselective excitation of Cr^{3+} at 532 nm, the luminescence decays show marked differences. The Tm^{3+} C_3 center emission starts almost immediately after pumping in Cr^{3+}, regardless of temperature and Tm^{3+} concentration, while that of C_1 and C_2 shows an obvious risetime dependent on these factors. Thus for the sample YAG: Cr (0.2 at. %), Tm (3.1 at. %) the risetime for C_3 at 77 K is of about 0.2 μs, which indicates a transfer rate inside the corresponding Cr^{3+}-Tm^{3+} pairs of the order of 2.5×10^7 s^{-1}. Such a fast transfer leads to a drastic shortening of the Cr^{3+} emission decay for these pairs: a very short emission drop of less than 100 ns was in fact observed at the beginning of Cr^{3+} emission decay at 300 K in garnets codoped by Cr^{3+} and Tm^{3+} or Er^{3+}.[26] Since the global deexcitation of Cr^{3+} in this case is much faster than that of Tm^{3+}, the decay portion of the temporal evolution of C_3 Tm^{3+} emission excitation in Cr^{3+} is determined by Tm^{3+} deexcitation processes. The emission decays of Tm^{3+} C_3 under selective pump in $^3F_3$ Tm^{3+} and quasiselective pump in R_2 Cr^{3+} are similar. Under nonselective pump at 532 nm, the temporal evolution of Tm^{3+} C_3 emission becomes more complex since this acceptor subsystem is also excited by distant transfer from the other donor subsystems including the nonperturbed subsystem D_n. The effect of this slow transfer is observed in the Tm^{3+} C_3 decay at 4.2 K as a bump in the 200–300 μs range; however the beginning of decay after pump at 532 nm at 77

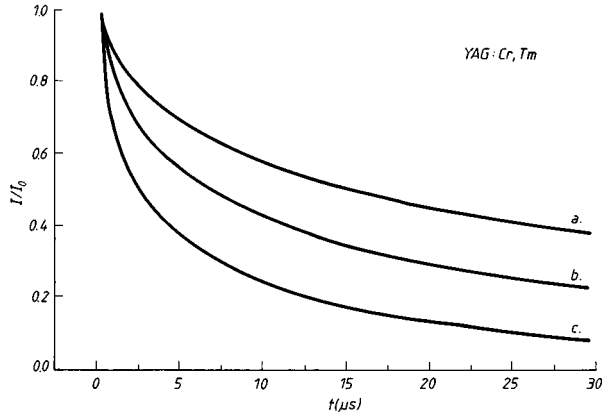

FIG. 2. $^3H_4$ normalized luminescence decay of C_3 Tm^{3+} center in YAG:Cr,Tm at 77 K under 532 nm excitation: (a) 3.1 at. % Tm; (b) 4.25 at. % Tm; (c) 6 at. % Tm.

K, shown in Fig. 2 for three samples of various Tm^{3+} concentrations, is similar to that obtained with selective pumping in $^3F_3$ Tm^{3+}.

The Cr^{3+}-Tm^{3+} energy transfer in case of the less-perturbed centers C_1 and C_2 is much slower: at 4.2 K the transfer rate is of several hundreds to thousands of s^{-1} (function on Tm^{3+} concentration), much smaller than the rate of intrinsic deexcitation of Tm^{3+}. For these centers, the Tm^{3+} emission under pump in Cr^{3+} shows a slow rise ($t_{A\,\max}$ for C_1 in the sample of 3.1 at. % Tm^{3+} is of about 150 μs), determined by the Tm^{3+} intrinsic deexcitation, followed by a slower decay determined by the Cr^{3+}-Tm^{3+} transfer. The low transfer rate for these centers is evident also from the Cr^{3+} emission decay whose long-time behavior indicates that for the more distant Cr^{3+}-Tm^{3+} pairs the transfer is even slower. Figure 3 presents the normalized $^3H_4$ emission decay of the N Tm^{3+} center at 77 K for three Tm^{3+} concentrations. These very large differences in the transfer rates for the resolved C_i Tm^{3+} centers influence also the value of the peak instantaneous transfer excited population, $n_{A\,\max}$, which is much larger for the center C_3 than for C_1 and C_2. Together with a possible enhancement of the emission transition probability for this center, due to the strong static perturbation, this could give a false picture

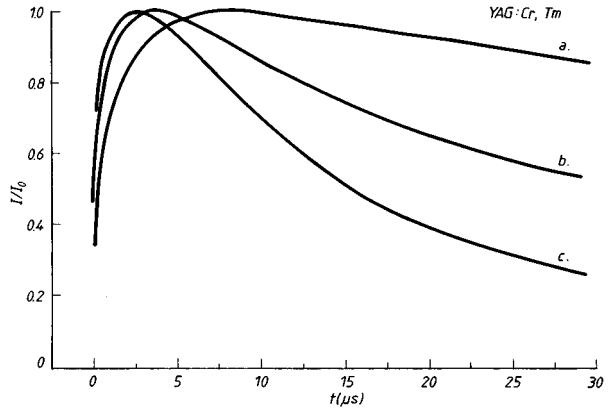

FIG. 3. $^3H_4$ normalized luminescence decay of N, main Tm^{3+} center in YAG:Cr,Tm in the same conditions as in Fig. 1.

of correlated (enhanced) placement of Cr^{3+} and Tm^{3+} ions for this center, especially when the emission spectrum is registered at early times (in the region of $t_{A\,\max}$ for C_3). However, the differences in the normalized total number of excited acceptors $n_{A\,\mathrm{tot}}$ for all these three perturbed centers are not so large.

The small shift of lines C_1 and C_2 from line N together with the larger Cr^{3+}-Tm^{3+} transfer rates for the former makes the observation of N emission under excitation in Cr^{3+} very difficult at low temperatures. Due to the loss of resolution, at high temperatures an emission with rise time strongly dependent on temperature and on Tm^{3+} concentration collects C_1, C_2, and N contributions. For the YAG sample with Cr (0.1 at. %), Tm (3.1 at. %), $t_{A\,\max}$ is of about 7.5 μs at 77 K and drops to 3 μs at 300 K. This shortening could be connected with a strong increase of the energy transfer with temperature (especially between 4.2 and 77 K). The transfer rates for C_1 and C_2 increase from $\sim 10^3\ s^{-1}$ at 4.2 K to $2\times 10^5\ s^{-1}$ at 77 K and $1.5\times 10^6\ s^{-1}$ at 300 K for the sample referred above. These values are characteristic for multipolar interactions between ions and the strong temperature dependence is due to the decrease of Cr^{3+} intrinsic lifetime and to the enhancement of the superposition integral of donor emission and acceptor absorption. However, in the case of C_3 the very high transfer rate over the entire temperature range suggests that the Cr-Tm interaction responsible for transfer is a superexchange.

Despite the drastic temperature enhancement of the Cr^{3+}-Tm^{3+} transfer rate for C_1 and C_2 (and N) centers, in most of the temperature range it still remains smaller than the intrinsic rate of Tm^{3+} deexcitation and thus it continues to determine the decay portion of temporal evolution of sensitized emission. However, for each Cr^{3+} and Tm^{3+} concentration, a specific temperature where these two processes interchange their role could be defined. The enhancement of $n_{A\,\max}$ and the reduction of $t_{A\,\max}$ with temperature as a consequence of the acceleration of the transfer makes the temporal behavior of the sensitized emission resemble gradually the behavior under pump in Tm^{3+}, especially at high dopant concentrations.

In case of Cr^{3+}-sensitized emission of Tm^{3+} in GGG where the spectral lines are broader than in YAG, only one new Tm^{3+} center was observed;[7] most probably it corresponds to the strongly perturbed center C_3 in YAG. An attempt to explain the behavior of Cr^{3+} and Tm^{3+} emission for these centers by taking into account various ion-ion interactions points out that the d-q and superexchange interaction could account for the high rate of transfer.

C. Fe^{3+} sensitization of Tm^{3+} emission in garnets

Unlike Cr^{3+} which enters only in octahedral a sites of garnets, Fe^{3+} could occupy the tetrahedral d sites too. An efficient energy transfer from $^4T_1(^4G)$ (first excited level) $Fe^{3+}(d)$ to the $^3H_4$ Tm^{3+} level was reported recently[9,10] for YAG and GGG. The Tm^{3+} emission excited by $Fe^{3+}(d)$ shows three Tm^{3+} satellites F_i in the Tm^{3+} $^3H_4(1)\rightarrow{}^3H_6(1)$ emission in both crystals. In YAG their position is at 794.71, 793.98, and 793.07 nm, respectively, (N is at 793.35 nm). For the most shifted centers F_1 and F_2, lines corresponding to the forbidden transition

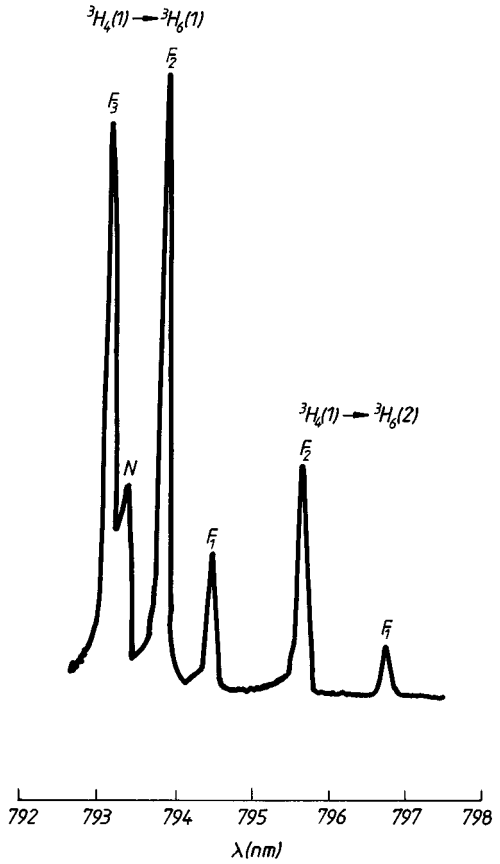

FIG. 4. Part of the $^3H_4\rightarrow{}^3H_6$ Tm^{3+} emission of a YAG: Fe(1 at. %), Tm(1 at. %) at about 5 μsec after excitation in $Fe^{3+}(d)$.

$^3H_4(1)\rightarrow{}^3H_6(2)$ in D_2 are also observed, showing a strong crystal-field perturbation. Figure 4 shows part of the Fe^{3+}-sensitized $^3H_4$ Tm^{3+} emission spectrum in a YAG sample containing Fe (1 at. % in melt) and Tm (1 at. %), registered at about 5 μs after pumping. The lines corresponding to forbidden transitions (in D_2) $^3H_4(1)\rightarrow{}^3H_6(2)$ for F_1 and F_2 are also observed. The emission spectrum for samples of different Fe^{3+} and Tm^{3+} concentrations are similar, but the relative intensities of satellite emission with respect to the line N changes. Symmetry and structure arguments suggest that these centers might be connected with the perturbing effect of Fe^{3+} situated in the first, second, and third d-coordination spheres, on the Tm^{3+} dodecahedral c site. Unlike Cr^{3+}, the perturbing effect of Tm^{3+} ions is observed in the Fe^{3+} spectra too by the presence of a satellite line in $^4T_2(^4D)$ absorption, the correspondent of the F_1 Tm^{3+} center. The observation of the three new F_i satellites in Tm^{3+} emission justifies again the division of Tm^{3+} and Fe^{3+} ion systems into four subsystems.

For both systems YAG:Cr,Tm, and YAG:Fe,Tm the excitation spectra in the Tm^{3+} levels of the perturbed centers show clear differences from the unperturbed center N, especially for the most perturbed centers C_3 and F_1, respectively. Thus the superposition integral between sensitizer emission (Cr or Fe) and activator absorption ($^3F_2$ and $^3F_3$ Tm^{3+} levels for the first system and $^3H_4$ for the second) show specific differences for each subsystem, leading to individual values of the energy-transfer microparameters C_{DA} for various ion-ion interactions.

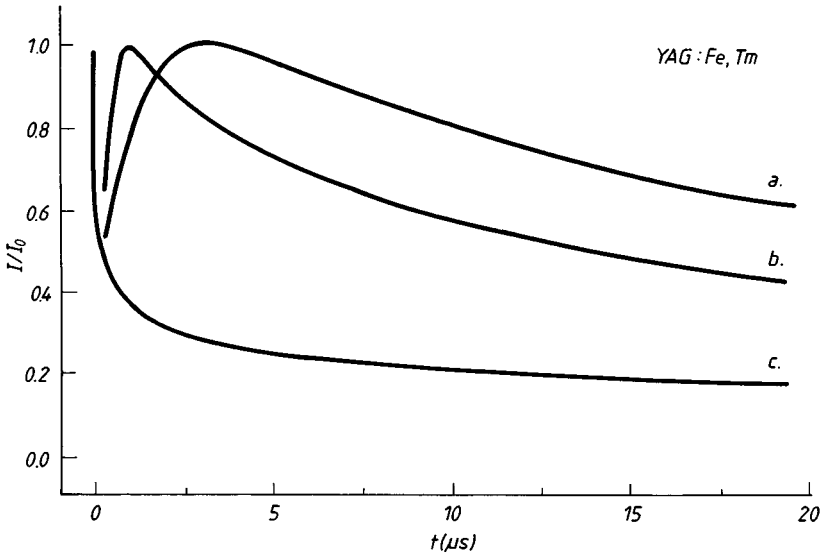

FIG. 5. $^3H_4$ normalized luminescence decay of (a) N, (b) F_3, and (c) F_1 centers at 77 K in YAG: Fe(1 at. %), Tm(5 at. %) under 532 nm excitation.

Since the shifts of the F_i satellites are larger than those of the C_i satellites described above, the dynamical behavior of these centers could be followed with a higher accuracy. The $Fe^{3+}(d)$-sensitized emission of all these centers in YAG:Fe,Tm shows rise time (dependent on concentration), but while for the perturbed centers $t_{A\,\max}$ is very short ($F_1 \sim 0.02$ μs, $F_2 \sim 0.04$ μs, $F_3 \sim 0.8$ μs for 5 at. % Tm^{3+} at 77 K), for center N it is about 4 μs for 5 at. % and 155 μs for 1 at. % Tm, see Fig. 5. This suggests large differences between the corresponding Fe^{3+}-Tm^{3+} transfer rates; manifested also in the value of $n_{A\,\max}$. The rise portion of the emission evolution is determined by $Fe^{3+}(d)$ deexcitation in case of the perturbed centers and by Tm^{3+} deexcitation for the N center. The temporal evolution indicates a strong dependence of the transfer rate on concentration and temperature. For the strongly perturbed center F_1 and possibly for F_2 the energy transfer is most probably dominated by superexchange, for F_3 the high-order multipolar interactions might be important, while for distant Fe^{3+}-Tm^{3+} pairs the coupling is dipolar. A correlation with the spectroscopic data shows that the main reason for the temperature dependence of the transfer microparameter is the modification of the superposition integrals. Due to a larger linewidth and to a poorer resolution, the data on GGG:Fe,Tm are less accurate than for YAG; they, however, confirm the general conclusion of the investigation of the latter.

IV. CONCLUSION

The present investigation demonstrates the essential connection between the mutual static crystal-field perturbations produced by the sensitizer and activator ions at each other's site and their dynamical behavior. Due to the discrete nature of these perturbations, as a result of the discrete placement of these ions in the lattice sites, the systems of sensitizer (D) and activator (A) ions become inhomogeneous: however they could be considered as composed of several homogeneous subsystems connected to specific D-A pairs whose effect is resolved in a given experiment, a special subsystem being composed from ions whose perturbation is not resolved (''isolated ions''). These subsystems are also personalized as concerns the energy transfer by a selective manifestation of the interactions responsible for transfer.

In laser crystals without correlation, the statistics of a discrete random and equiprobable occupancy of the sites enable the calculation of the probability of occurrence of each subsystem for given D and A concentrations. A rate equation modeling which accounts for the energy transfer via a transfer function calculated for this model of discrete substitution enables the calculation of the temporal evolution of the excited populations for each of the donor and acceptor subsystems.

This model was tested for the case of YAG:Tm^{3+} sensitized with Cr^{3+} (in octahedral sites) or Fe^{3+} (in tetrahedral sites) and a good description of the emission $^3H_4$ temporal behavior after excitation in the donor systems was obtained for all the resolved subsystems. This modeling shows that the large differences in energy-transfer processes for each of these systems determine the variety in their emission temporal evolution. This study shows that the activator emission in sensitized laser crystals could present large differences from emission in the absence of the sensitizer. This conclusion could be important for the modeling of laser processes especially for those which use laser-pulsed excitation. Such processes could be general for sensitized crystals and they could change completely the emission characteristics especially at high dopant concentrations; such a case can be considered in GSGG:Nd,Cr (GSGG is gadolinium scandium gallium garnet),[11] where the main emission wavelength is shifted to a perturbed subsystem for a ratio between the sensitizer and activator concentrations of 8:1. Unfortunately, many spectroscopic studies on the laser crystals neglect completely these aspects and this reduces considerably the data for an accurate modeling of the emission processes.

[1] D. L. Dexter, J. Chem. Phys. **21**, 836 (1953).
[2] T. Forster, Ann. Phys. **2**, 55 (1948).
[3] M. Inokuti and F. Hirayama, J. Chem. Phys. **43**, 1978 (1965).
[4] I. S. Golubov and Y. V. Konobeev, Sov. Phys. Solid State **13**, 2679 (1972).
[5] A. Mares, Z. Khas, W. Nie, and G. Boulon, J. Phys. (France) I **1**, 881 (1992).
[6] W. Nie, Y. Kalisky, Ch. Pedrini, A. Monteil, and G. Boulon, Opt. Quant. Electron **22**, S123, (1990).
[7] A. Brenier, G. Boulon, C. Pedrini, and C. Madej, Opt. Mater. **1**, 224 (1992).
[8] V. Lupei, L. Lou, G. Boulon, A. Lupei, and C. Tiseanu, J. Phys. (France) I **3**, 1245 (1993).
[9] V. Lupei, G. Boulon, A. Lupei, M. J. Elejalde, A. Brenier, and C. Pedrini, J. Lumin. **60/61**, 241 (1994).
[10] V. Lupei, G. Boulon, A. Lupei, M. J. Elejalde, A. Brenier, and C. Pedrini, Phys. Rev. B **49**, 7076 (1994).
[11] T. P. J. Han, M. A. Scott, F. Jaque, H. G. Gallagher, and B. Henderson, Chem. Phys. Lett. **208**, 63 (1993).
[12] V. Lupei, A. Lupei, and G. Boulon, J. Phys. (France) IV **4**, 305 (1994).
[13] E. W. Dubinski, G. Huber, and P. M. Mitzerlich, *Topical Meeting on Tunable Solid State Lasers (OSA)* [Tech. Digest **80-3**, 11 (1986)].
[14] T. Becker and G. Huber, J. Phys. (France) IV **1**, 353 (1991).
[15] G. Armagan, B. Di Bartolo, and A. M. Buoncristiani, J. Lumin. **44**, 129 (1989); **44**, 141 (1989).
[16] J. B. Gruber, M. E. Hills, R. M. Macfarlane, C. A. Morrisou, G. A. Turner, J. Q. Quarless, J. K. Kintz, and L. Esterowits, Phys. Rev. B **40**, 9464 (1989).
[17] A. Lupei, C. Tiseanu, and V. Lupei, Phys. Rev. B **47**, 14 084 (1993).
[18] C. Tiseanu, A. Lupei, and V. Lupei, J. Phys. Condens. Matter **7**, 8477 (1995).
[19] V. Lupei, A. Lupei, and G. Boulon, J. Phys. (France) IV **4**, 407 (1994).
[20] V. V. Osiko, Yu. K. Voronko, and A. A. Sobol, *Crystals* (Springer-Verlag, Berlin, 1984), Vol. 10, p. 37.
[21] N. Y. Agladze, H. S. Bagdasarov, E. A. Vinogradov, V. I. Zhekov, T. M. Murina, N. N. Popova, and E. A. Fedov, *Kristallografia* **33**, 913 (1988).
[22] V. Lupei, A. Lupei, S. Georgescu, and C. Ionescu, Opt. Commun. **60**, 59 (1986).
[23] V. Lupei, A. Lupei, C. Tiseanu, S. Georgescu, C. Stoicescu, and P. M. Nanau, Phys. Rev. B **51**, 8 (1995).
[24] A. Lupei, H. Gross, and P. Reike, J. Phys. Condens. Matter **7**, 5701 (1995).
[25] Yu. K. Voronko, S. B. Gessen, N. A. Eskov, A. A. Kirykhin, P. A. Ryabochkina, A. A. Sobol, V. M. Tatarintsev, S. N. Ushakov, and L. I. Tsymbal, Quant. Electron. **23**, 958 (1993).
[26] I. T. Sorokina, J. Phys. (France) IV **4**, C4-521 (1994).